XIV International Conference on Computational Plasticity. Fundamentals and Applications
COMPLAS 2017
E. Oñate, D.R.J. Owen, D. Peric and M. Chiumenti (Eds)

FEM Analysis on Fundamental Relationship between Hydrostatic Stress and Strain Obtained from Uniaxial Tensile Test Using Axially symmetric Tapered Specimen

Hiromu Sakamoto*, Takashi Iizuka†

* Department of Mechanical and System Engineering
Kyoto Institute of Technology
Matsugasaki Goshokaido-cho, Sakyo-ku, Kyoto 606-8585, Japan
E-mail: m7623111@edu.kit.ac.jp

† Faculty of Mechanical Engineering
Kyoto Institute of Technology
Matsugasaki Goshokaido-cho, Sakyo-ku, Kyoto 606-8585, Japan
E-mail: tiizuka@kit.ac.jp

Key words: FEM analysis, Tensile properties, Axially symmetric tapered specimen, Forming limit

Abstract. In sheet metal forming, we can recognize most deformed states by using in-plane biaxial deformation and can predict the occurrence of fracture by a forming limit diagram. However, in the case of axially symmetric tensile specimens, it is known that the magnitude of hydrostatic stress or stress triaxiality largely affects the occurrence of fracture. In this study, we investigated the history of hydrostatic stress and stress triaxiality by using an axially symmetric tapered tensile specimen.

1 INTRODUCTION

In sheet metal forming, it is very important to understand the forming limit for various in-plane strain paths [1], [2]. A method to obtain a forming limit diagram was decided in the ISO standard [3]. However, the changes in hydrostatic stress depend on the strain path. It is known that the magnitude of hydrostatic stress largely affects the occurrence of fracture. Therefore, to evaluate the forming limit for each strain path more precisely, a new evaluation method considering hydrostatic stress would be beneficial. With a new method to test the uniaxial tension state, various hydrostatic stress states could be differentiated by using axially symmetric specimens of various shapes. However, few studies have investigated new methods. Thus, in this study, we used axially symmetric tapered tensile specimens to evaluate the forming limit of the uniaxial tension state in various hydrostatic stress states.

Using finite element method (FEM) analyses, we investigated the hydrostatic stress-strain responses for elastic and plastic deformation of axially symmetric tapered tensile specimens during the uniaxial tensile test. By changing the taper angle, the possibility to control the hydrostatic stress in tensile tests was also examined.

In the elastic deformation region, it was found that the hydrostatic stress could be controlled by changing the taper angle of the axially symmetrical specimen. The hydrostatic stress

increased with increasing taper angle. In the plastic deformation region, the hydrostatic stress at the center of the specimen varied nonlinearly. The nonlinear curve of hydrostatic stress and equivalent stress became larger by increasing the taper angle. Trials of varying taper angles were conducted to correlate the equivalent strain to the hydrostatic stress, and possible methods were considered to evaluate the forming limit at various hydrostatic stress states by using axial symmetry tapered specimens.

2 THEORY

2.1 Relationship between hydrostatic stress and pre-strain

According to Ohji [4], hydrostatic stress does not affect occurrence of void; however, the stress largely affects the growth of a void. He also concluded that, as the strain grows, the void is stretched in the axial direction rather than in the radial direction. Therefore, it seems that hydrostatic stress after the occurrence of a void affects the growth of the void and the occurrence of fracture. Figure 1 shows the relationship between hydrostatic stress and pre-strain. Here, we define σ as stress and ε as strain.

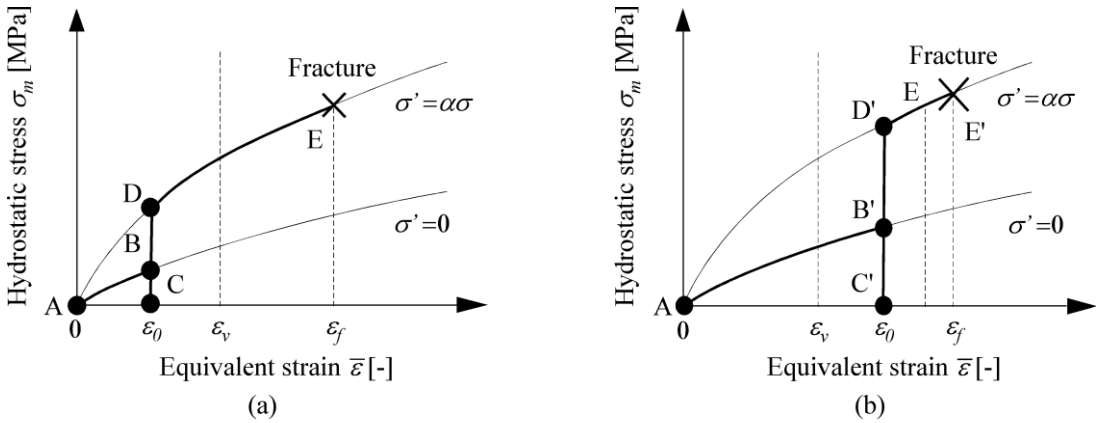

Figure 1: Relationship between hydrostatic stress and equivalent strain
(a) Pre-strain $\varepsilon_0 < \varepsilon_v$, (b) Pre-strain $\varepsilon_0 > \varepsilon_v$

In Figure 1, we define ε_0 as pre-strain, ε_v as equivalent strain when void is caused and ε_f as fracture equivalent strain. Figure 1 (a) shows ε_0 is smaller than ε_v. Figure 1 (b) shows ε_0 is larger than ε_v. It appears that ε_f in Figure 1 (b) is larger than ε_f in Figure 1 (a), because hydrostatic stress affects the growth of the void.

2.2 Relationship between stress triaxiality and equivalent strain

According to Oyane [5], the relative density of the material of a specimen decreases due to void growth during deformation. He proposed criteria for ductile fracture based on the relative density of the material. To predict the forming limit, Takuda [6] proposed criteria for ductile fracture using the following equation, which is used along with finite element analysis.

$$I = \frac{1}{b}\int_0^{\varepsilon_f}\left(\frac{\sigma_m}{\bar{\sigma}} + a\right)d\bar{\varepsilon} \tag{1}$$

In equation (1), the integral value I is composed of equivalent strain and stress triaxiality. Stress triaxiality is given by the following equation in the case of $\sigma_1>\sigma_2=\sigma_3$ by assuming uniaxial tensile test. We can judge fracture when the integral value I becomes 1. The stress triaxiality in equation (2) is given in equation (3) by assuming $\sigma_2=\sigma_3=0$, i.e., using non-tapered specimen, or equation (4) by assuming $\sigma_2 = \sigma_3 = \alpha\bar{\sigma}$, i.e., using tapered specimen.

$$\frac{\sigma_m}{\bar{\sigma}} = \frac{\sigma_1 + \sigma_2 + \sigma_3}{3\bar{\sigma}} = \frac{1}{3} + \frac{\sigma_2}{\bar{\sigma}} \tag{2}$$

$$\frac{\sigma_m}{\bar{\sigma}} = \frac{1}{3} \tag{3}$$

$$\frac{\sigma_m}{\bar{\sigma}} = \frac{1}{3} + \alpha \tag{4}$$

Figure 2 shows relationship between stress triaxiality and equivalent strain.

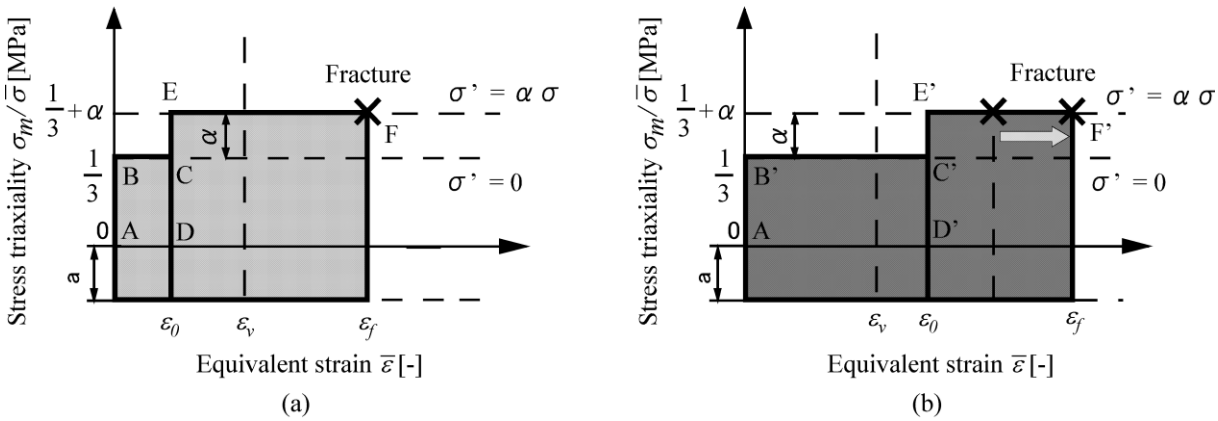

Figure 2: Relationship between stress triaxiality and equivalent strain
(a) Pre-strain $\varepsilon_0 < \varepsilon_v$, (b) Pre-strain $\varepsilon_0 > \varepsilon_v$

In Figure 2, the gray area in Figure 2 (b) is larger than that in (a). Therefore, ε_{fb} is larger than ε_{fa}.

2.3 Relation between stress triaxiality and pre-strain

Similarly to hydrostatic stress, stress triaxiality affects the growth of a void. Therefore, we can rewrite equation 1) as follows by changing the integration range when the void is caused by ε_v.

$$I' = \frac{1}{b'} \int_{\varepsilon_v}^{\varepsilon_f} \left(\frac{\sigma_m}{\bar{\sigma}} + a' \right) d\bar{\varepsilon} \tag{5}$$

Figure 3 shows the relationship between equations 3), 4) and 5).

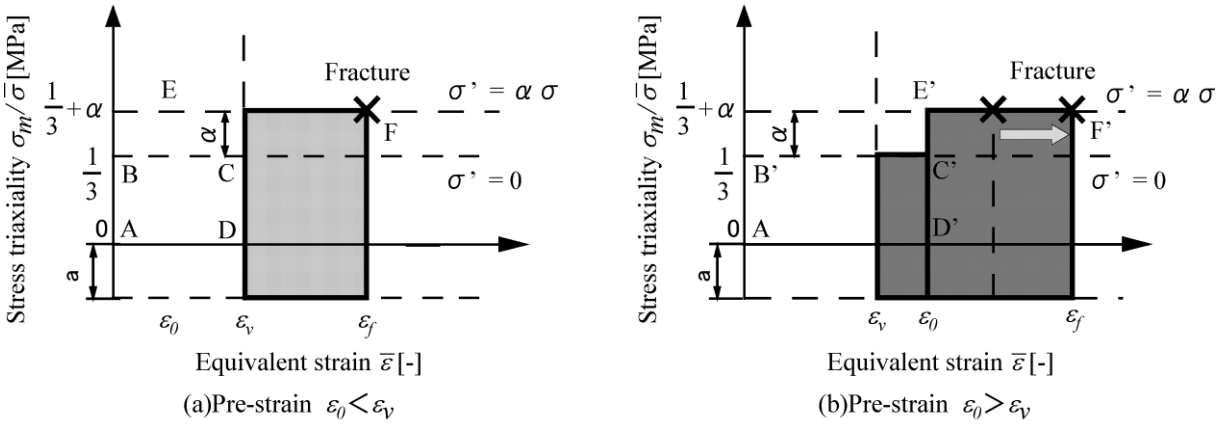

Figure 3: Relationship between stress triaxiality and equivalent strain after occurrence of void (a) Pre-strain $\varepsilon_0 < \varepsilon_v$, (b) Pre-strain $\varepsilon_0 > \varepsilon_v$

Figure 2 shows that ε_{fb} is larger than ε_{fa}.

3 EXPERIMENT

3.1 Experimental conditions

An experiment was conducted with axially symmetric tensile specimens made of aluminum (A1070). Figure 4 shows the specimen shape before the axial tensile test to give pre-strain.

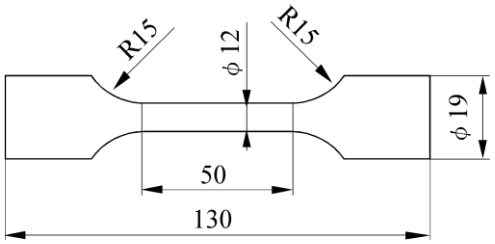

Figure 4: Specimen for pre-straining

The axial tensile test is conducted with the specimen in Figure 4. Figure 5 shows the load-stroke curve.

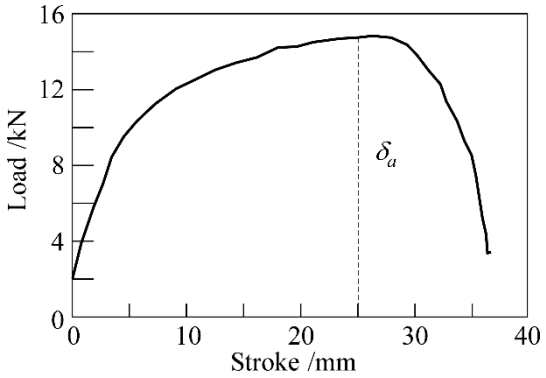

Figure 5 : Tensile test to give pre-strain

In Figure 5, the void caused at stroke = 25 mm is due to necking. Therefore, from the result of the tensile test, the specimen is pre-strained when the stroke is 25 mm. The value of the pre-strain is 0.05413. Furthermore, the specimen shape is changed by additional process. Figure 6 shows the specimen shapes after processing. Here, θ is tapered angle in Figure 6 (b).

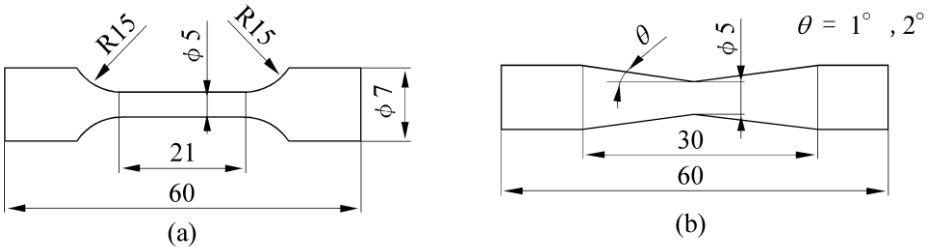

Figure 6: Specimen before and after pre-straining and processing (a) Non-tapered (b) Tapered

3.2 Experimental results

Figure 7 shows the fracture surfaces after the axial tensile test with specimen in Figure 6.

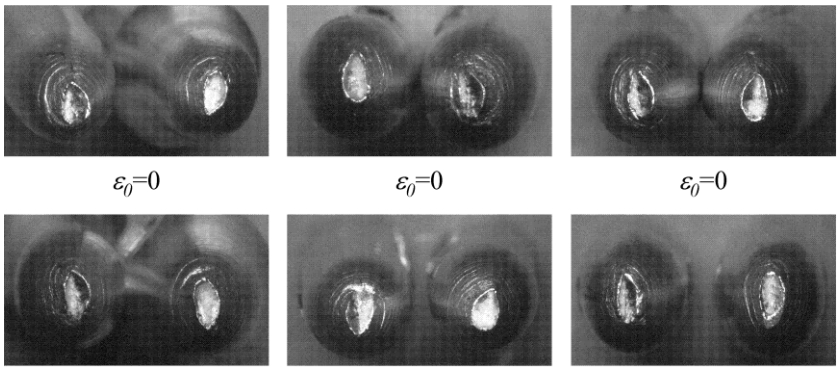

Figure 7 : The fracture surface (a)θ=0° (b)θ=1° (c)θ=2°

In Figure 7, all surfaces are cup and cup. Therefore, it seems that the void is stretched in the axial direction in the tensile test. The fracture point is at the center of the specimen in Figure 7 (b), where θ=1° and Figure 7 (c), where θ=2°. However, the fracture point is not at the center of the specimen in Figure 7 (a), where θ=0°. The fracture equivalent strain can be calculated by the following equation. Here, we define A_0 as cross-sectional area before tensile test and A as it after tensile test.

$$\varepsilon_{eq}' = -\ln\left(\frac{A}{A_0}\right) \tag{6}$$

The fracture equivalent strains are listed in Table 1.

Table 1: Fracture strain before and after axially symmetric tensile test

Fracture strain	θ=0°	θ=1°	θ=2°
$\varepsilon_0 = 0$	2.458	2.250	2.165
$\varepsilon_0 = 0.05413$	2.340	2.195	1.949

4 ANALYSIS

4.1 Analytical condition

The analysis is conducted by simfact forming. Figure 9 shows the analysis model and Table 2 shows the analysis condition.

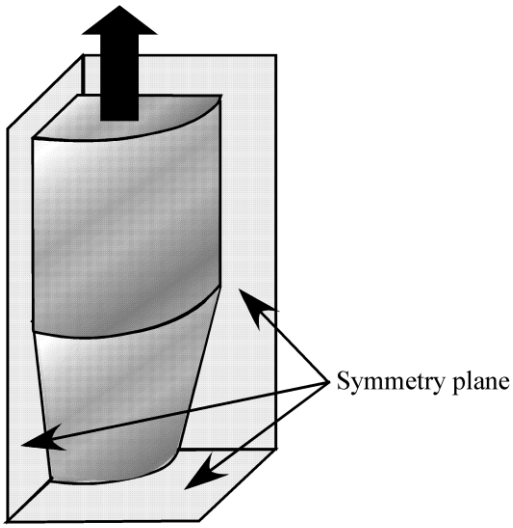

Figure 8 : 1/8 specimen model

Table 2: The material should be the first listed

Flow curve	$\sigma = F\varepsilon^n$
Young's modulus / GPa	71
Poisson's ratio	0.33
Material	A1070
Pre-strain	0
Work hardening exponent	0.0161
Plastic coefficient / MPa	119

In Figure 8, the 1/8 symmetry model is used to reduce the analytical time and expense. However, the tensile part has a fine mesh in order to observe the area in detail. In Table 2, the

mechanical properties were calculated using a tensile test. In the analysis of the axial tensile test, the data output interval was 0.005 mm, and the equivalent strain at the center of the specimen was 3.0.

4.2 Analytical results

Figure 9 shows the relationship between equivalent strain and hydrostatic stress or stress triaxiality.

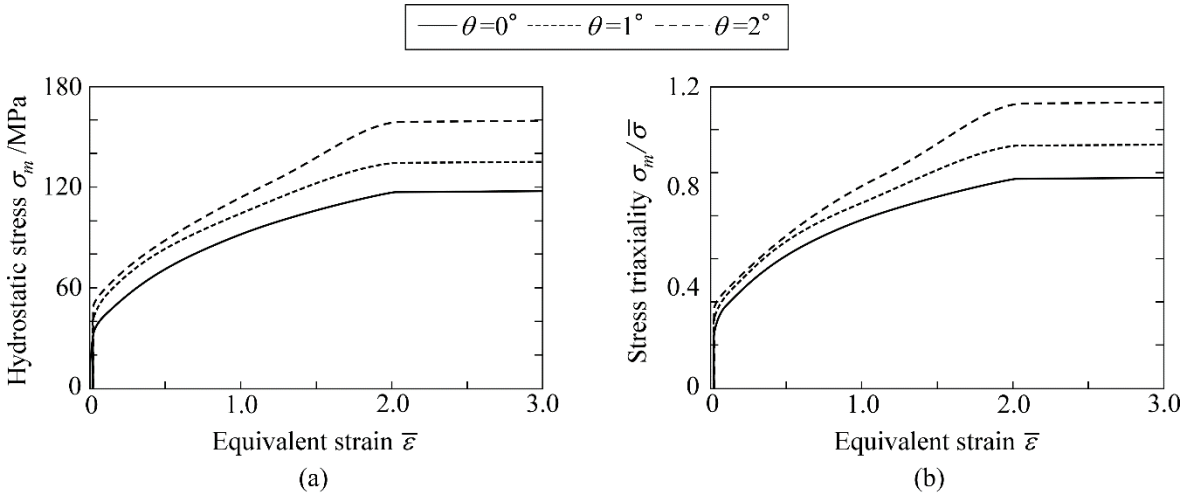

Figure 9 : Relationship between equivalent strain and (a) hydrostatic stress (b) stress triaxiality

In Figure 9, hydrostatic stress and stress triaxiality increase with increasing taper angle. Therefore, the stress states at the center of the specimen are changed by the taper angle. Furthermore, in the plastic deformation region, hydrostatic stress at the center of the specimen varies nonlinearly. The nonlinear curve of hydrostatic stress and equivalent stress becomes larger with increasing taper angle.

5 CONCLUSIONS

- In the experiment, unlike the theory, the fracture equivalent strain of a specimen with pre-strain is smaller than it is without pre-strain.
- The work-hardening exponent of the material in this study is very small. Therefore, the uniform elongation region is very short in the tensile test. Essentially, the material needs to have uniform deformation in the length region. Furthermore, the void grows too large because the stroke in the tensile test is excessive for pre-straining a specimen. Detailed observation of the specimen cross section during the tensile test is required.
- In the analysis, the results suggest a possible method to evaluate the forming limit at various hydrostatic stress states by using axially symmetry tapered specimens.

REFERENCES

[1] C. Karadogan, M.E. Tamer, “Development of a new and simplified procedure for the experimental determination of forming limit curves”, CIRP annuals, 64, 265-268, (2015).
[2] Y. Hanabusa, H. Takizawa, T. Kuwabara, “Evaluation of accuracy of stress measurements determined in biaxial stress tests with cruciform specimen using numerical method”, Steel Research International, 81, 1376-1379, (2010). Y. Hanabusa, H. Takizawa, T. Kuwabara, “Evaluation of accuracy of stress measurements determined in biaxial stress tests with cruciform specimen using numerical method”, Steel Research International, 81, 1376-1379, (2010).
[3] ISO 12004-2:2008(E).
[4] K. Ohji, K Ogura, Y. Mutoh, “The effect of hydrostatic pressure on the basic mechanisms of ductile fracture”, Transactions of the JSME, 42, 31-37, (1976).
[5] M. Oyane, “On criteria for ductile fracture”, Transactions of the JSME, 75, 596-601, (1972).
[6] H. Takuda, K. Mori, T. Hirose, N. Hatta, “Prediction of Forming Limit in Axisymmetric Deep Drawing of Steel/Aluminium Alloy Laminated Sheets Using a Simple Criterion for Ductile Fracture”, Journal of Japan Society for Technology of Plasticity, 37, 509-514, (1996).